ChemComm

Reactive two-component monolayers template bottom-up assembly of nanoparticle arrays on HOPG

Journal:	*ChemComm*
Manuscript ID	CC-COM-05-2018-004058.R1
Article Type:	Communication

ChemComm

COMMUNICATION

Reactive two-component monolayers template bottom-up assembly of nanoparticle arrays on HOPG †

Received 00th January 20xx,
Accepted 00th January 20xx

DOI: 10.1039/x0xx00000x

www.rsc.org/

Chen Fang, Hua Zhu, Ou Chen and Matthew B. Zimmt*

Two triphenyleneethynylene derivatives, 1^{OH} and 2, self-assemble a patterned monolayer (ML) at the solution - graphite (HOPG) interface. The four molecule unit cell of the ML, ($1^{OH}1^{OH}22$), spans 19 nm and contains adjacent columns of 1^{OH} molecules spaced by 4.7 nm. Following ML assembly, a disulfide is appended to the reactive group on each 1^{OH} molecule and used to capture 2.0 nm gold nanoparticles (AuNP). The patterned monolayer directs bottom-up assembly of a 5 nm / 19nm double pitch AuNP pattern.

Designed monolayers (ML) expressing compositional patterns assemble spontaneously on planar surfaces from multi-component solutions.[1,2,3,4,5] Incorporating distinct reactivity in the components of pattered monolayers should allow these assemblies to function as ultra-high resolution templates.[6,7] Surfaces with controlled nanometer spacing of nano-objects, e.g. biomolecules nano-particles, and surface grown polymers, could find use in electronic, optical, magnetic or analytical applications given their unique structures. Assembly of surfaces with designed patterns of different size nanoparticles has been demonstrated on mica[8] using DNA Origami.[9] Nanoparticle capture on polymer[10] or physisorbed monolayer surfaces afford various levels of organization, from random[11] to well aligned assemblies,[12,13,14] albeit with minimal pattern control. A related strategy underlies directed self-assembly lithography, which yields features with sub-10 nm pitch.[15,16,17] Here we employ time of flight mass spectrometry (TOF-MS) and scanning probe microscopies (STM, AFM) to demonstrate the self-assembly, chemical functionalization and application of a two-component patterned monolayer as a template to direct gold nanoparticle (AuNP) surface assembly into columns with 5 nm and 19 nm spacing patterns. Extending this strategy to the growing number of multi-component ML systems[1-7] will enable bottom-up fabrication of increasingly complex nano-object assemblies.

Two triphenyleneethynylene (TPE) molecules, $\mathbf{1}^{OH}$ and **2** (Fig. 1), were designed to assemble monolayers comprised of two adjacent columns of $\mathbf{1}^{OH}$ molecules alternating with two adjacent columns of **2** molecules (($1^{OH}1^{OH}22$) unit cell). $\mathbf{1}^{OH}$ and **2** contain long side chains with different shapes and lengths to direct self-assembly of the patterned ML morphology. Molecule $\mathbf{1}^{OH}$ has one "linear" docosyloxy side chain, [23], and one "bumped" heptacosa-11,13,20,22-tetrayn-1-yloxy side chain, [28out], attached at opposing terminal para-positions of a TPE unit. The central benzene ring of $\mathbf{1}^{OH}$ has two "core chains"; a methoxy group ortho to the aryl ring bearing the [23] side chain and a 6-hydroxyhex-1-yloxy chain ortho to the aryl ring bearing the [28out] side chain. The terminal hydroxyl group on the $\mathbf{1}^{OH}$ chain is the site of ML reaction and template function. Molecule **2** has a "linear" hexadecyloxy side chain, [17], and a "bumped" heptacosa-5,7,14,16-tetrayn-1-yloxy side chain [28in] at opposing para-positions of the TPE. The central benzene ring of **2** has two hexyloxy core chains para to each other.

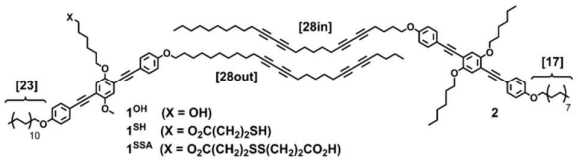

Fig.1 Structures of TPE compounds, $\mathbf{1}^{OH}$ and **2**, used to self-assemble patterned mono-layers (ML) with a four molecule unit cell, ($1^{OH}1^{OH}22$). Reactions at the ML - solution interface convert $\mathbf{1}^{OH}$ into $\mathbf{1}^{SSA}$, $\mathbf{1}^{SH}$ and $\mathbf{1}^{SS}\mathbf{1}$ (not shown).

The TPE molecules' two long side chains extend in opposite directions. These side chains assemble aliphatic lamella by interdigitating with shape- and length-complementary side chains from an adjacent column of TPE units. Close packing of comple-mentary side chains within aliphatic lamellae generates van der Waals interactions that stabilize ML assembly and the intended morphology. Segregation of [17] and [23] chains into separate lamellae maximizes van der Waals interactions for both side chains. Interdigitation of identical length [17] side chains drives assembly of two adjacent columns of **2** molecules. Likewise, interdigitation of [23] side chains directs assembly of analogous "double columns" of $\mathbf{1}^{OH}$ molecules. The off-center locations of the "tetrayne-bumps" in [28in] and [28out] make this side chain pair shape-complementary but make each side chain shape self-incommensurate. Aliphatic lamellae containing tetrayne-bump chains attain maximum van der Waals stabilization by packing each [28] chain between two copies

Department of Chemistry, Brown University, Providence, RI 02912 USA.
E-mail: mbz@brown.edud

† Electronic Supplementary Information (ESI) available: [General protocols, Synthesis of AuNP, $\mathbf{1}^{OH}$ and **2**, statistical summaries of MS intensities from independent samples, TOF-MS from each spot sampled on each drop cast ML and on each ML formed following surface reactions, STM and AFM images of ($1^{OH}1^{OH}22$) monolayer after DBTP modification and AuNP incubation]. See DOI: 10.1039/x0xx00000x

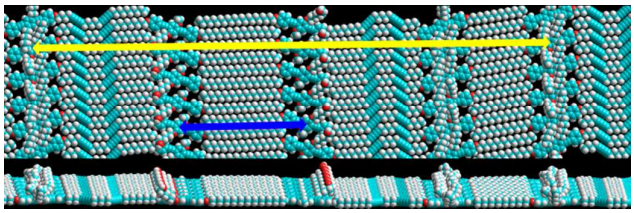

Fig. 2. Top: Molecular mechanics minimized section of ($\mathbf{1}^{OH}\mathbf{1}^{OH}\mathbf{22}$) morphology ML on HOPG. The unit cell repeat spans 18.8 nm (yellow arrow). The center-to-center distance between nearest $\mathbf{1}^{OH}$ columns is 4.7 nm (blue arrow). Bottom: ML section side view.

of the other [28] chain. This directs assembly of $\mathbf{1}^{OH}$ and **2** columns on opposite edges of each tetrayne chain lamella. Molecular mechanics modeling predicts the ($\mathbf{1}^{OH}\mathbf{1}^{OH}\mathbf{22}$) morphology separates the centers of TPE units in adjacent $\mathbf{1}^{OH}$ columns by 4.7 nm. The unit cell repeat (Fig. 2) enforces a separation of 18.8 nm between the centers of neighboring $\mathbf{1}^{OH}$ "double columns".

Monolayers of $\mathbf{1}^{OH}$ and **2** were assembled on highly oriented pyrolytic graphite (HOPG) from equimolar solutions in phenyloctane (5-20 µM each compound). Scanning tunneling microscopy (STM) images collected from the solution - HOPG interface revealed assembly of two different ML morphologies (Fig. 3a). The dominant morphology exhibited the desired ($\mathbf{1}^{OH}\mathbf{1}^{OH}\mathbf{22}$) pattern, with a ML repeat containing four aliphatic lamellae. The second morphology, observed infrequently and with poor resolution, exhibited only two aliphatic lamellae per repeat, one of which was narrower than any aliphatic column in the ($\mathbf{1}^{OH}\mathbf{1}^{OH}\mathbf{22}$) patterned morphology. The incidence of this minor morphology varied from sample to sample. Surprisingly, phenyloctane solutions of $\mathbf{1}^{OH}$ applied to HOPG exhibited MLs in STM scans, despite the absence of the shape complementary bumped-tetrayne side chain from **2**. MLs assembled from $\mathbf{1}^{OH}$ solutions exhibited the same lamellar pattern (Fig. S1, ESI) as the minor morphology assembled from equimolar solutions of $\mathbf{1}^{OH}$ and **2**. The two long side chains on $\mathbf{1}^{OH}$ ([23] and [28out]) afford this molecule a physisorption advantage, enabling it to assemble single component ML domains in competition with the two component, patterned domains. Adjusting $\mathbf{1}^{OH}$ and **2** concentrations and ratios might counteract this advantage so that only the ($\mathbf{1}^{OH}\mathbf{1}^{OH}\mathbf{22}$) morphology assembles (vide infra).

STM must be used to verify morphologies assembled by multi-component ML, but this technique samples small areas (< 1 µm^2) and is slow. Time-of-flight mass spectrometry (TOF-MS) rapidly analyses much larger areas of MLs assembled on HOPG[18] (> 2000 µm^2 per irradiated spot), providing relative compositions of multi-component ML convolved with a response factor for each component.[19] Solution preparation conditions that assemble only the patterned ($\mathbf{1}^{OH}\mathbf{1}^{OH}\mathbf{22}$) morphology ML should produce the same, constant value of the $\mathbf{1}^{OH}$:**2** TOF-MS intensity ratio. TOF-MS can rapidly screen ML composition as a function of different $\mathbf{1}^{OH}$ and **2** solution concentrations to identify promising solution mixtures. STM can then be used to ascertain the specific ML morphology assembled by these mixtures. Accordingly, $\mathbf{1}^{OH}$:**2** TOF-MS intensity

Table 1. $\mathbf{1}^{OH}$: **2** Surface TOF-MS Intensity Ratio versus Solution Composition

[$\mathbf{1}^{OH}$]:[**2**] Solution Ratio →	2 : 1	1 : 1	1 : 1.5	1 : 2
[$\mathbf{1}^{OH}$] = 4 µM	1.01±0.37	0.51±0.11	0.42±0.06	0.40±0.07
[$\mathbf{1}^{OH}$] = 3 µM	0.81±0.24	0.45±0.08	0.43±0.07	0.41±0.06

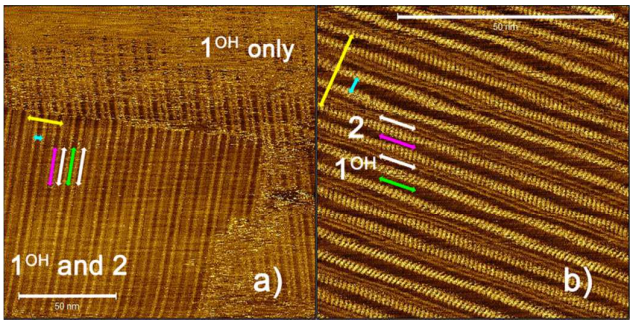

Fig. 3. STM images of drop cast $\mathbf{1}^{OH}$ / **2** ML on HOPG. Arrows mark features of the ($\mathbf{1}^{OH}\mathbf{1}^{OH}\mathbf{22}$) patterned domains: the 19 nm repeat (yellow), the center-to-center distance between nearest $\mathbf{1}^{OH}$ columns (cyan), [17] lamella (magenta), bumped tetrayne lamella (white), [23] lamella (green). Scale bars are 50 nm wide. a) ML drop cast from 10 µM $\mathbf{1}^{OH}$ / 10 µM **2** solution (160 nm x 160 nm) contains both patterned (lower left) and $\mathbf{1}^{OH}$-only domains. b) ML drop cast from 4 µM $\mathbf{1}^{OH}$ and 6 µM **2** solution (72 nm x 72 nm) contains only the ($\mathbf{1}^{OH}\mathbf{1}^{OH}\mathbf{22}$) patterned morphology.

ratios were determined at multiple locations of HOPG substrates prepared from various $\mathbf{1}^{OH}$ and **2** solution concentrations and ratios.

Samples for TOF-MS analyses were prepared by applying 6 µL of $\mathbf{1}^{OH}$ / **2** solution on freshly cleaved HOPG (12 mm x 12 mm) at 19 °C. After sitting 15 minutes, the HOPG substrate was rinsed with 25 µL of phenyloctane to remove non-adsorbed TPE and then with hexane (3 x 25 µL) to remove phenyloctane. A thin film of the MALDI matrix 2,4,6-trihydroxyacetophenone (THAP) was applied (15 µL 1.7 mg/ml THAP in 30% acetone/octane solution) to the HOPG substrate to increase TOF-MS signal intensities. TOF-MS determined $\mathbf{1}^{OH}$:**2** ion[20] intensity ratios (Table 1, Fig. 4, Fig. S2 ESI) exhibited a plateau value of 0.42 for applied phenyloctane solutions containing 3 or 4 µM $\mathbf{1}^{OH}$ and 50-100% higher **2** concentrations (4.5 - 8 µM).[21] Larger and more variable $\mathbf{1}^{OH}$:**2** TOF-MS intensity ratios arose from samples prepared using higher concentrations of $\mathbf{1}^{OH}$ (e.g. 10 µM) or higher relative concentrations of $\mathbf{1}^{OH}$ (equimolar or higher). These latter solutions assembled ML on HOPG with "excess" $\mathbf{1}^{OH}$. This concurs with STM observation of single component $\mathbf{1}^{OH}$ domains in addition to patterned ($\mathbf{1}^{OH}\mathbf{1}^{OH}\mathbf{22}$) domains from equimolar $\mathbf{1}^{OH}$ / **2** phenyloctane solutions. STM images of ML prepared by drop casting 4 µM $\mathbf{1}^{OH}$ / 6 µM **2** solutions exhibited patterned ($\mathbf{1}^{OH}\mathbf{1}^{OH}\mathbf{22}$) domains (Fig. 3b) but no evidence of single component $\mathbf{1}^{OH}$ domains.[21] This solution composition was used to prepare ML for AuNP template studies.

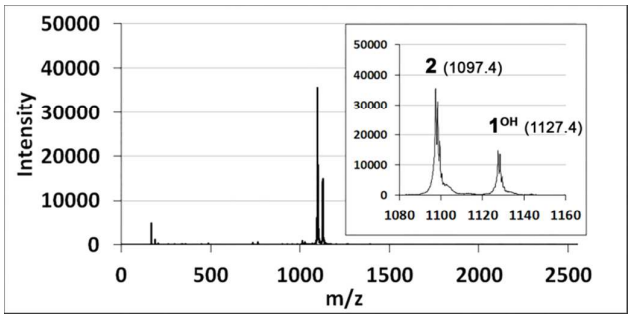

Fig. 4. TOF-MS of ML assembled on HOPG from 6 µL phenyloctane containing 6 µM **2** and 4 µM $\mathbf{1}^{OH}$. A thin THAP film (m/z = 169 $[M+H]^+$) was applied to the ML to increase signal intensities. Inset: expansion of the **2** and $\mathbf{1}^{OH}$ peak region. This sample's $\mathbf{1}^{OH}$: **2** intensity ratio is 0.42.[21] See Fig. S2 ESI for all TOF-MS data from drop cast solutions.

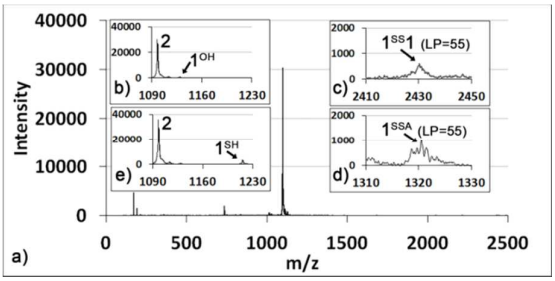

Fig. 5. TOF-MS after surface reactions and application of thin THAP film. a) Spectrum (0-2.5kD, laser power =47%) after esterifcation of $\mathbf{1}^{OH}$ with DTBP. b) Expansion of a) showing reduced intensity of $\mathbf{1}^{OH}$ after DTBP surface reaction. c) TOF-MS (laser power = 55%) of dimer region after DTBP surface reaction. d) TOF-MS (laser power = 55%) of $\mathbf{1}^{SSA}$ region after DTBP surface reaction. e) TOF-MS (laser power = 47%) of monomer region after DTT reduction of DTBP esterified ML.

Following assembly of the patterned ($\mathbf{1}^{OH}\mathbf{1}^{OH}\mathbf{22}$) ML, the terminal hydroxyl group of $\mathbf{1}^{OH}$ was reacted with 3,3'-dithiobis-propanoic acid (DTBP) to install a disulfide group on this core chain ($O(CH_2)_6O_2C(CH_2)_2$S-S-R) and enable capture of AuNP. Steglich esterification[22] using DTBP can i) cross-link $\mathbf{1}^{OH}$ molecules within the same TPE column, forming dimeric TPE_2 linked by a disulfide, $\mathbf{1}^{SS}\mathbf{1}$, or ii) form a core chain containing a disulfide group and a terminal carboxylic acid, $\mathbf{1}^{SSA}$ (Fig. 1). Patterned ($\mathbf{1}^{OH}\mathbf{1}^{OH}\mathbf{22}$) ML on HOPG was incubated twelve hours in dimethylformamide (DMF) solution containing 20 mM DTBP, 40 mM 1-(3-dimethylaminopropyl)-3-ethylcarbodiimide hydrochloride (EDC) and 40 mM dimethylamino-pyridine (DMAP). The HOPG substrate was then rinsed with DMF (2 x 0.25 mL), water (0.5 mL) and ethanol (2 x 0.1 mL) to remove reagents, by-products and to dry the ML. TOF-MS spectra collected after applying a thin THAP film (Fig. 5a-b, Fig. S3 ESI) exhibited normal intensity from **2** (ion intensity ~ $3x10^4$) but less than 5% of the previous $\mathbf{1}^{OH}$ intensity ($\mathbf{1}^{OH}$:**2** int. ratio = 0.02±0.01). TOF-MS measurements at higher laser power, required to detect heavier and less intense species,[23] revealed (Fig. 5c-d, Fig. S4 ESI) a low intensity peak at m/z ~ 2432 assigned as TPE_2 $\mathbf{1}^{SS}\mathbf{1}$ (ion intensity < 600) and a low intensity peak at m/z = 1320. assigned as $\mathbf{1}^{SSA}$ (ion intensity < 1000).[20] TPE_2 dimers adhere more strongly to HOPG than TPE monomers.[19] Comparable TOF-MS intensities from $\mathbf{1}^{SS}\mathbf{1}$ and $\mathbf{1}^{SSA}$ indicates ML cross-linking competes favourably with "bimolecular" reaction between solution DTBP and $\mathbf{1}^{OH}$ in the ML.[24] DTBP reacted ML were not imageable by STM.[25]

The dimeric nature of the $\mathbf{1}^{SS}\mathbf{1}$ peak was confirmed by reduction of the disulfide cross-link with dithiothreitol (DTT).[26] DTBP-reacted ML was incubated with DTT for three hours (50 mM DTT, pH=7.8 0.2M Tris buffer, 1.5 mL). After rinsing with water (2 x 0.25 mL) and drying, a thin THAP film was applied and TOF-MS spectra collected. The peaks attributed to $\mathbf{1}^{SS}\mathbf{1}$ and $\mathbf{1}^{SSA}$ were absent (Fig. S5 ESI). A new peak observed at m/z = 1216. (Fig. 5e, Fig. S5 ESI) was assigned as $\mathbf{1}^{SH}$, a TPE bearing a ($O(CH_2)_6O_2C(CH_2)_2$SH), thiol-terminated core chain (Fig. 1). [20] The $\mathbf{1}^{SH}$ peak intensity was roughly 10% as large as the non-reactive ML molecule **2** ($\mathbf{1}^{SH}$:**2** int. ratio = 0.11±0.01). This intensity ratio was much smaller than the starting $\mathbf{1}^{OH}$:**2** ratio (0.42), which could indicate loss of $\mathbf{1}^{OH}$ derived compounds due to cross-linking. To estimate relative TOF-MS response factors for $\mathbf{1}^{SH}$ and **2**, the former was prepared from patterned ($\mathbf{1}^{OH}\mathbf{1}^{OH}\mathbf{22}$) ML by a route that avoided cross-linking. The ($\mathbf{1}^{OH}\mathbf{1}^{OH}\mathbf{22}$) ML was esterified using the mono-ethyl ester of 3,3'-dithiobispropanoic[27] and reduced with

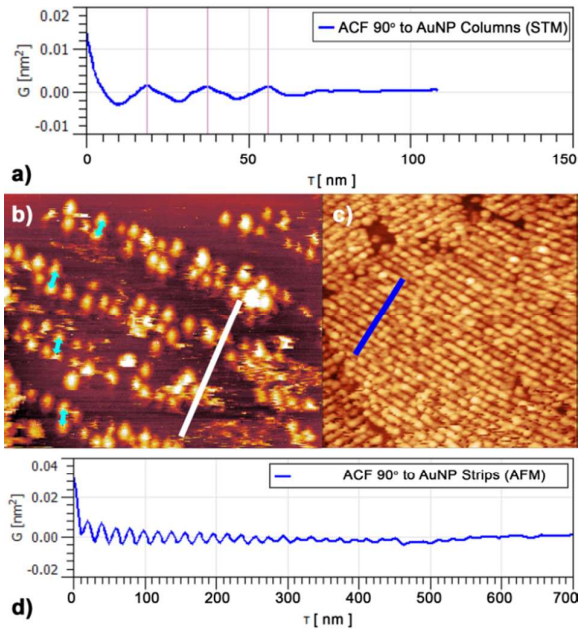

Fig. 6. a) 1-D height autocorrelation function (ACF)[30] of STM image perpendicular to AuNP columns (white bar in b). Pink lines mark maxima at 18.8, 37.6 and 56.1 nm. b) STM image (100 nm x 75 nm) of DTBP reacted ($\mathbf{1}^{OH}\mathbf{1}^{OH}\mathbf{22}$) ML after incubation with 2 nm AuNP. Cyan arrows mark 5 nm. c) 0.6μM x 0.6 μM AFM image of DTBP modified ($\mathbf{1}^{OH}\mathbf{1}^{OH}\mathbf{22}$) ML after incubation with 2 nm AuNP. The bright strips are captured AuNP. d) 1-D height autocorrelation function (ACF)[30] of AFM image perpendicular (blue bar in c) to the AuNP strips. Maxima are spaced by 20±1 nm.

DTT using the procedures described above. The $\mathbf{1}^{SH}$:**2** int. ratio generated by this surface reaction, 0.09±0.01 (Fig. S6, ESI), was similar to the ratio following reduction of DTBP cross-linked ML. This indicates reasonable retention of $\mathbf{1}^{OH}$ compounds during cross-linking and a four-fold smaller response factor for $\mathbf{1}^{SH}$ than for $\mathbf{1}^{OH}$.[28]

For AuNP capture studies, ($\mathbf{1}^{OH}\mathbf{1}^{OH}\mathbf{22}$) ML was esterified with DTBP to install disulfide groups on $\mathbf{1}^{OH}$ columns and then incubated with 2 nm diameter AuNP. AuNP stabilized with oleylamine surface coatings[29] were used; the weak amine - gold bond should facilitate reactive capture of AuNP by ML disulfide groups. Patterned ML were incubated for 15-60 minutes in hexane (1 mL) containing 5 μg of AuNP and then rinsed, dropwise, with 2 mL of hexane. STM images (MS-10 STM, Veeco) displayed AuNP patterns consistent with the designed ML template. High resolution STM scans (Fig. 6b) resolved double AuNP columns, with ~ 5 nm spacing of the proximate AuNP columns. The scan's 1-D height autocorrelation function (ACF)[30] (Fig. 6a) perpendicular to the AuNP columns in the STM image exhibit maxima at intervals of ~ 19 nm. Less distinct shoulders are present at distances ~ 5 nm shorter and longer than the 18.8 and 37.6 nm maxima. Both features are consistent with the double column morphology of the underlying ($\mathbf{1}^{OH}\mathbf{1}^{OH}\mathbf{22}$) ML. Additional STM images (Fig. S7, ESI) confirmed assembly of AuNP columns with the 5nm / 19nm double column morphology

Large area tapping mode AFM images (MFP-3D Origin, Asylum Research) collected at the air - HOPG interface (Fig. 6c) revealed roughly linear strips spaced by 20±1 nm, with 10±2 nm FWHM and 1.5 - 2 nm height modulation. The strips are assigned as AuNP templated by the ML as no comparable features were observed in AFM images collected from ($\mathbf{1}^{OH}\mathbf{1}^{OH}\mathbf{22}$) MLs on HOPG or from

(**1**^{OH}**1**^{OH}**22**) MLs exposed to AuNP without DTBP modification.[31] The radius of the AC240TS-R3 AFM probe (7 nm) did not afford sufficient resolution to verify that each strip is composed of double AuNP columns spaced by 5 nm. AFM visualized domains contained 10 - 30 parallel strips and approached 500 nm in length, albeit with breaks. The 1-D height autocorrelation function (ACF) [30] orthogonal to the AuNP strip direction exhibited more than fifteen maxima spaced by 19 - 20 nm. Strip orientations in adjacent domains differed by ~60^{o}, indicating that the underlying HOPG symmetry axes control alignment of AuNP assemblies by directing (**1**^{OH}**1**^{OH}**22**) ML domain orientations.[32] The AFM studies confirm ML mediated, bottom-up assembly of AuNP structures with a 19 nm repeat.

In conclusion, STM and TOF-MS were used to identify preparation conditions that optimize self-assembly of (**1**^{OH}**1**^{OH}**22**) patterned MLs. Patterned ML assembly was driven by length and shape dependent interactions of TPE side chains. TOF-MS was used to verify the subsequent covalent modification of **1**^{OH} molecules with a disulfide group at the ML - solution interface. STM and AFM imaging demonstrated that disulfide modified MLs effectively translate patterned ML morphology into a bottom-up template, directing surface assembly of AuNP into 5-nm spaced doubled columns with an overall 19 nm repeat. Efforts to apply self-patterned MLs as high resolution templates directing patterned surface assembly of multiple NP components is ongoing.

This work was supported by the U.S. National Science Foundation grant number CHE1607273. Assistance with mass spectrometry from Dr. Tun-Li Shen, Ken Talbot and Randy Goulet, with NMR from Dr. Hopson and with AFM from Dr. Hector Garces is acknowledged gratefully.

Notes and references

[1] J. A. Theobald, N. S. Oxtoby, M. A. Phillips, N. R. Champness and P. H. Beton, *Nature*, **2003**, *424*, 1029–1031.
[2] G. Velpula, T. Takeda, J. Adisoejoso, K. Inukai, K.Tahara, K. S. Mali, Y. Tobe and S. De Feyter, *Chem. Commun.,* **2017**, *53*, 1108-1111.
[3] Z.-F. Cai, T. Chen, J.-Y. Gu, D. Wang and L.-J. Wan, *Chem. Commun*., **2017**, *53*, 9129-9132.
[4] Y. Xue and M. B. Zimmt, *J. Am. Chem. Soc*., **2012**, *134*, 4513–4516.
[5] A. Ciesielski, C.-A. Palma, M. Bonini, and P. Samori, *Adv. Mater*., **2010**, *22*, 3506-20.
[6] Y. L. Huang, W. Chen and A. T. S. Wee, *J. Am. Chem. Soc*., **2011**, *133*, 820–825.
[7] K. Tahara, K. Nakatani, K. Iritani, S. De Feyter and Y. Tobe, *ACS Nano*, **2016**, *10*, 2113-2120.
[8] Y. Y. Pinto, J. D. Le, N. C. Seeman, K. Musier-Forsyth, T. A. Taton, and R. A. Kiehl, *Nano Lett*., **2005**, *5*, 2399–2402.
[9] P. W. K. Rothemund, *Nature*, **2006**, *440*, 297-302.
[10] R. Shenhar, T. B. Norsten and V. M. Rotello, *Adv. Mater.* **2005**, *17*, 657-669.
[11] X. Wei, W. Tong, V. Fidler and M. B. Zimmt, *J. Colloid Interf. Sci.*, **2012**, 221-227.
[12] M. A. Mezour, I. I. Perepichka, J. Zhu, R. B. Lennox and D. F. Perepichka, *ACS Nano*, **2014**, *8*, 2214-2222.
[13] S.-B. Lei, C. Wang, S.-X. Yin, L.-J. Wan and C.-L. Bai, *Chem. Phys. Chem*, **2003**, *4*, 1114-1117.
[14] J.-U. Kim, K.-H. Kim, N. Haberkorn, P. J. Roth, J.-C. Lee, P. Theato and R. Zentel, *Chem. Commun*., **2010**, *46*, 5343–5345.
[15] M. R. Bockstaller, Y. Lapetnikov, S. Margel and E. L. Thomas, *J. Am. Chem. Soc.*, **2003,** *125*, 5276-5277
[16] C. Park, J. Yoon and E. L. Thomas, *Polymer*, **2003**, *44*, 6725-6760.
[17] S.-M. Park, X. Liang, B. D. Harteneck, T. E. Pick, N. Hiroshiba, Y. Wu, B. A. Helms and D. L. Olynick, *ACS Nano*, **2011**, *5*, 8523–8531.
[18] J. He, C. Fang, R. A. Shelp and M. B. Zimmt, *Langmuir*, **2017**, *33*, 459–467.
[19] J. He, K. J. Myerson and M. B. Zimmt, *Chem. Commun*., **2018**, *46*, 3636–3639.
[20] The (monoisotopic, average, observed) m/z values for the ML compounds analyzed in this study are **1**^{OH} (1126.8, 1127.7, 1127.5); **2** (1096.8, 1097.7, 1097.5); **1**^{SH} (1214.8, 1215.9, 1215.7); **1**^{SSA} (1318.8, 1320.0, 1320.5), **1**^{SS}**1** (2428.7, 2429.7, 2432).
[21] A compound's MS-TOF signal intensity depends on its desorption / ionization efficiencies and on its propensity to fragment. STM observation of excess **1**^{OH} in ML prepared from equimolar **1**^{OH} / **2** solutions indicates stronger physisorption of **1**^{OH} than **2** to HOPG. Stronger **1**^{OH} adhesion contributes to the MS-TOF **1**^{OH}:**2** plateau value, 0.42, from (**1**^{OH}**1**^{OH}**22**) patterned MLs being less than one.
[22] B. Neises, W. Steglich, *Angew. Chem. Int. Ed*., **1978**, *17*, 522-524.
[23] A laser power setting of 47% was used to quantify **1**^{OH} : **2** ratios, as neither compound's ion intensity approached saturation levels (ion counts of > 75,000) at this power. A laser power setting of 55% was needed to detect **1**^{SSA} and **1**^{SS}**1**, presumably due to their low surface concentration and heavy mass, respectively. The ion intensity from **2** reached saturation at this laser power, making ion intensity ratios relative to **2** unreliable. Laser power settings above 55% increased fragmentation of the tetrayne chains.
[24] Esterification using 5-fold higher DTBP concentration (100 mM), two-fold lower EDC (20 mM) and the same DMAP concentration (40 mM) gave 4.5-fold higher **1**^{SSA} intensity and 10% lower **1**^{SS}**1** intensity (Fig. S4, ESI). The large increase of "bimolecular product", **1**^{SSA}, but minimal change to cross-linked product, **1**^{SS}**1**, at the higher DTBP concentration demonstrates that cross-linking is faster than (competitive with) "bimolecular" reaction at 20 mM DTBP concentration.
[25] STM scans of TPE ML with polar groups on core chain termini (attached in-situ or ex-situ) exhibit excessive scratches (e.g. Fig. 3a).
[26] W. W. Cleland*, Biochemistry,* **1964**, *3*, 480-482.
[27] For the preparation of (3-((3-ethoxy-3-oxopropyl)disulfaneyl)-propanoic acid) see J. Zhao, Y. Zhou, Y. Li, X. Pan, W. Zhang, N. Zhou, K. Zhang, Z. Zhang and X. Zhu, Polym. Chem., 2015, 6, 2879–2891.
[28] The 4-fold smaller response factor from **1**^{SH} compared to **1**^{OH} derives from the larger mass of **1**^{SH} and/or from additional fragmentation pathways.
[29] See the ESI for AuNP preparation, TEM and diameter histogram.
[30] The plots display height fluctuation autocorrelation functions. D. Nečas, P. Klapetek, "Gwyddion: An open-source software for SPM data analysis", *Cent. Eur. J. Phys*., **2012**, *10*, 181-188.
[31] See ESI Fig. S7 for AFM scans of these control experiments.
[32] The (**1**^{OH}**1**^{OH}**22**) MLs exhibit 2D-enantiomerism. The unit cell angle (between the TPE intra- and inter-column vectors) is ~87^{o}. Thus, enantiomeric domains aligned along the same HOPG symmetry axis have slightly non-parallel TPE lamellae and associated AuNP strips.

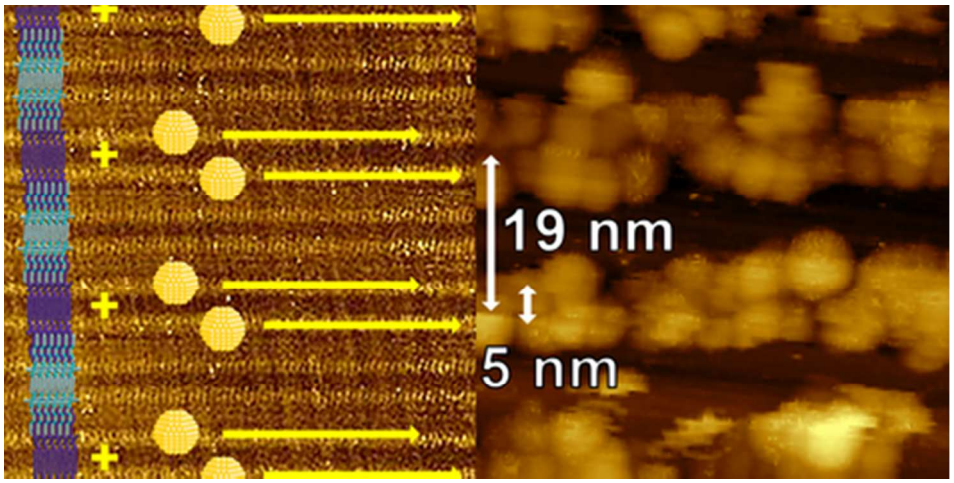

39x19mm (300 x 300 DPI)